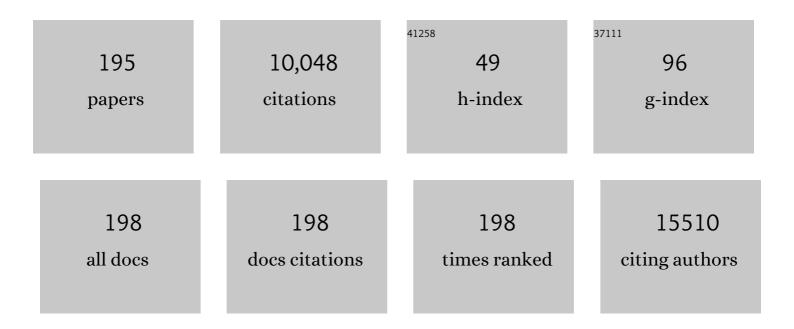


List of Publications by Year in descending order

Source: https://exaly.com/author-pdf/6801385/publications.pdf Version: 2024-02-01



#	Article	IF	CITATIONS
1	Energy Band Alignment and Redoxâ€Active Sites in Metalloporphyrinâ€Spaced Metalâ€Catechol Frameworks for Enhanced CO ₂ Photoreduction. Angewandte Chemie, 2022, 134, .	1.6	3
2	Energy Band Alignment and Redoxâ€Active Sites in Metalloporphyrinâ€Spaced Metalâ€Catechol Frameworks for Enhanced CO ₂ Photoreduction. Angewandte Chemie - International Edition, 2022, 61, .	7.2	23
3	Top gate engineering of field-effect transistors based on wafer-scale two-dimensional semiconductors. Journal of Materials Science and Technology, 2022, 106, 243-248.	5.6	11
4	Tailoring atomic 1T phase CrTe ₂ for in situ fabrication. Nanotechnology, 2022, 33, 085302.	1.3	5
5	Rigid-Foldable Mechanism Inspired by Origami Twisted Tower. Journal of Mechanisms and Robotics, 2022, 14, .	1.5	2
6	An in situ digital background calibration algorithm for multi-channel R-βR ladder DACs. Journal of Electronic Science and Technology, 2022, 20, 100150.	2.0	2
7	Gamma-ray polarimetry of the Crab pulsar observed by <i>POLAR</i> . Monthly Notices of the Royal Astronomical Society, 2022, 512, 2827-2840.	1.6	5
8	Engineering Top Gate Stack for Wafer-Scale Integrated Circuit Fabrication Based on Two-Dimensional Semiconductors. ACS Applied Materials & Interfaces, 2022, 14, 11610-11618.	4.0	9
9	The Trends of In Situ Focused Ion Beam Technology: Toward Preparing Transmission Electron Microscopy Lamella and Devices at the Atomic Scale. Advanced Electronic Materials, 2022, 8, .	2.6	6
10	Recent advances in ethanol gas sensors based on metal oxide semiconductor heterojunctions. Rare Metals, 2022, 41, 1818-1842.	3.6	71
11	Highâ€performance flexible humidity sensors for breath detection and nonâ€ŧouch switches. Nano Select, 2022, 3, 1168-1177.	1.9	10
12	Grapheneâ€Based Hydrogel Strain Sensors with Excellent Breathability for Motion Detection and Communication. Macromolecular Materials and Engineering, 2022, 307, .	1.7	7
13	Atomistic Observation of the Local Phase Transition in MoTe ₂ for Application in Homojunction Photodetectors. Small, 2022, 18, e2200913.	5.2	12
14	Underwater contactless wet-mateable connector using bowl-shaped coils. Journal of Power Electronics, 2022, 22, 1176-1187.	0.9	3
15	Nanoscale Analysis of Breakdown Induced Crack Propagation in DTSCR Devices. , 2022, , .		0
16	Effect of low-frequency optical phonons on the thermal conductivity of <mml:math xmlns:mml="http://www.w3.org/1998/Math/MathML"><mml:mrow><mml:mn>2</mml:mn><mml:mi>Hmolybdenum disulfide. Physical Review B, 2022, 105, .</mml:mi></mml:mrow></mml:math 	ıi> ₄/m ml:r	nrœw>
17	The Trend of 2D Transistors toward Integrated Circuits: Scaling Down and New Mechanisms. Advanced Materials, 2022, 34, e2201916.	11.1	37

¹⁸ Stacking monolayers at will: A scalable device optimization strategy for two-dimensional semiconductors. Nano Research, 2022, 15, 6620-6627.

5.8 4

#	Article	IF	CITATIONS
19	Review of electrical stimulus methods of <i>in situ</i> transmission electron microscope to study resistive random access memory. Nanoscale, 2022, 14, 9542-9552.	2.8	4
20	Flexible Pressure Sensor Array with Multi-Channel Wireless Readout Chip. Sensors, 2022, 22, 3934.	2.1	0
21	Enhanced Removal of Hydrophobic Short-Chain <i>n</i> -Alkanes from Gas Streams in Biotrickling Filters in Presence of Surfactant. Environmental Science & Technology, 2022, 56, 10349-10360.	4.6	30
22	An in Situ Embedded System for Electrocardiography and Photoplethysmography Acquisition. , 2022, , .		0
23	Waterproof and Breathable Grapheneâ€Based Electronic Fabric for Wearable Sensors. Advanced Materials Technologies, 2022, 7, .	3.0	8
24	Enhancement of the ferroelectricity by interface engineering observed by in situ transmission electron microscope. Applied Physics Letters, 2022, 120, .	1.5	2
25	High Throughput In–Situ Temperature Sensor Array with High Sensitivity and Excellent Linearity for Wireless Body Temperature Monitoring. Small Structures, 2022, 3, .	6.9	5
26	Directly integrated mixedâ€dimensional van der Waals graphene/perovskite heterojunction for fast photodetection. InformaÄnÃ-Materiály, 2022, 4, .	8.5	18
27	Structural properties of grain boundary in graphene grown on germanium substrates with different orientations. Applied Physics Letters, 2022, 121, 011901.	1.5	1
28	Design of Hybrid Zeolitic Imidazolate Frameworkâ€Derived Material with C–Mo–S Triatomic Coordination for Electrochemical Oxygen Reduction. Small, 2021, 17, e2003256.	5.2	14
29	A novel gradient thermoelectric microwave power sensors based on GaAs MMIC technology. Microsystem Technologies, 2021, 27, 243-249.	1.2	6
30	Atomically defined Co on two-dimensional TiO2 nanosheet for photocatalytic hydrogen evolution. Chemical Engineering Journal, 2021, 420, 127681.	6.6	40
31	Thermo-mechanical correlation in two-dimensional materials. Nanoscale, 2021, 13, 1425-1442.	2.8	53
32	Analog Sensing and Computing Systems with Low Power Consumption for Gesture Recognition. Advanced Intelligent Systems, 2021, 3, 2000184.	3.3	19
33	A template-free method to synthesis high density iron single atoms anchored on carbon nanotubes for high temperature polymer electrolyte membrane fuel cells. Nano Energy, 2021, 80, 105534.	8.2	35
34	Infrared Gesture Recognition System Based on Near-Sensor Computing. IEEE Electron Device Letters, 2021, 42, 1053-1056.	2.2	8
35	A hybrid zeolitic imidazolate framework-derived ZnO/ZnMoO ₄ heterostructure for electrochemical hydrogen production. Dalton Transactions, 2021, 50, 11365-11369.	1.6	7
36	Rational assembly of metal-oxo clusters into molecular materials <i>via</i> a "wheel mounting― mode. Inorganic Chemistry Frontiers, 2021, 8, 4102-4106.	3.0	0

#	Article	IF	CITATIONS
37	Object Identification With Smart Glove Assembled by Pressure Sensors. , 2021, 5, 1-4.		4
38	Pressure Sensor Array With Low-Power Near-Sensor CMOS Chip for Human Gait Monitoring. , 2021, 5, 1-4.		8
39	End-Bonded Contacts of Tellurium Transistors. ACS Applied Materials & Interfaces, 2021, 13, 7766-7772.	4.0	12
40	Vertically Aligned MoS ₂ with In-Plane Selectively Cleaved Mo–S Bond for Hydrogen Production. Nano Letters, 2021, 21, 1848-1855.	4.5	63
41	Direct Visualization of Breakdown-Induced Metal Migration in Enhanced Modified Lateral Silicon-Controlled Rectifiers. IEEE Transactions on Electron Devices, 2021, 68, 1378-1381.	1.6	8
42	VSe2 quantum dots with high-density active edges for flexible efficient hydrogen evolution reaction. Journal Physics D: Applied Physics, 2021, 54, 214006.	1.3	6
43	Facile fabrication of paper-based flexible thermoelectric generator. Npj Flexible Electronics, 2021, 5, .	5.1	41
44	Engineering the Coordination Sphere of Isolated Active Sites to Explore the Intrinsic Activity in Single-Atom Catalysts. Nano-Micro Letters, 2021, 13, 136.	14.4	138
45	Recent advances in flexible sweat glucose biosensors. Journal Physics D: Applied Physics, 2021, 54, 423001.	1.3	22
46	Recent Advances on Transition Metal Dichalcogenides for Electrochemical Energy Conversion. Advanced Materials, 2021, 33, e2008376.	11.1	114
47	Engineering hydrogels with homogeneous mechanical properties for controlling stem cell lineage specification. Proceedings of the National Academy of Sciences of the United States of America, 2021, 118, .	3.3	28
48	NS-MD: Near-Sensor Motion Detection With Energy Harvesting Image Sensor for Always-On Visual Perception. IEEE Transactions on Circuits and Systems II: Express Briefs, 2021, 68, 3078-3082.	2.2	7
49	CVD-Grown 2D Nonlayered NiSe as a Broadband Photodetector. Micromachines, 2021, 12, 1066.	1.4	3
50	A revew of in situ transmission electron microscopy study on the switching mechanism and packaging reliability in non-volatile memory. Journal of Semiconductors, 2021, 42, 013102.	2.0	6
51	Asymmetric metal–organic frameworks with double helices for enantioselective recognition. CrystEngComm, 2021, 23, 4748-4751.	1.3	3
52	A 10Ânm Short Channel MoS ₂ Transistor without the Resolution Requirement of Photolithography. Advanced Electronic Materials, 2021, 7, 2100543.	2.6	9
53	Construction of Hierarchical αâ€Fe ₂ O ₃ /SnO ₂ Nanoball Arrays with Superior Acetone Sensing Performance. Advanced Materials Interfaces, 2021, 8, 2001831.	1.9	18
54	Metal Migration Induced Breakdown from Gate Contact in Bulk FinFET Devices. , 2021, , .		0

#	Article	IF	CITATIONS
55	Failure Analysis on Diode-triggered Silicon-Controlled Rectifiers By using Nondestructive X-ray Microscopy. , 2021, , .		1
56	Agglomeration and removal characteristics of fine particles from coal combustion under different turbulent flow fields. Journal of Environmental Sciences, 2020, 89, 113-124.	3.2	19
57	Subnanometer iron clusters confined in a porous carbon matrix for highly efficient zinc–air batteries. Nanoscale Horizons, 2020, 5, 359-365.	4.1	27
58	Dual-defect surface engineering of bimetallic sulfide nanotubes towards flexible asymmetric solid-state supercapacitors. Journal of Materials Chemistry A, 2020, 8, 24053-24064.	5.2	133
59	Room temperature ferromagnetism in ultra-thin van der Waals crystals of 1T-CrTe2. Nano Research, 2020, 13, 3358-3363.	5.8	175
60	Printable and Flexible Planar Silver Electrodes-Based Resistive Switching Sensory Array. Frontiers in Sensors, 2020, 1, .	1.7	3
61	In Situ Interfacial Sublimation of Zn ₂ GeO ₄ Nanowire for Atomic-Scale Manufacturing. ACS Applied Nano Materials, 2020, 3, 4747-4754.	2.4	8
62	In Situ Dynamic Manipulation of Graphene Strain Sensor with Drastically Sensing Performance Enhancement. Advanced Electronic Materials, 2020, 6, 2000269.	2.6	23
63	Synthesis and photocatalytic activities of two homochiral metal–organic frameworks with cages and hydrogen bonding helices. CrystEngComm, 2020, 22, 4206-4209.	1.3	8
64	Ferromagnetic CoSe broadband photodetector at room temperature. Nanotechnology, 2020, 31, 374002.	1.3	15
65	Iron-doped VSe2 nanosheets for enhanced hydrogen evolution reaction. Applied Physics Letters, 2020, 116, .	1.5	18
66	Role of Optical Phonons in Bulk Molybdenum Diselenide Thermal Properties Probed by Advanced Raman Spectroscopy. Physica Status Solidi (B): Basic Research, 2020, 257, 2000251.	0.7	3
67	Tuning Electrical and Optical Properties of MoSe ₂ Transistors via Elemental Doping. Advanced Materials Technologies, 2020, 5, 2000307.	3.0	15
68	Effect of fluorine doping and sulfur vacancies of CuCo2S4 on its electrochemical performance in supercapacitors. Chemical Engineering Journal, 2020, 390, 124643.	6.6	132
69	Efficient perovskite solar cells <i>via</i> surface passivation by a multifunctional small organic ionic compound. Journal of Materials Chemistry A, 2020, 8, 8313-8322.	5.2	68
70	Strain engineering and lattice vibration manipulation of atomically thin TaS ₂ films. RSC Advances, 2020, 10, 16718-16726.	1.7	4
71	Thermal reliability study of graphene-based planar RRAM. , 2020, , .		0

72 Reliability study of flexible sodium-ion detection sensor. , 2020, , .

0

#	Article	IF	CITATIONS
73	HZIF-based hybrids for electrochemical energy applications. Nanoscale, 2019, 11, 15763-15769.	2.8	18
74	One-step synthesis of oxygen-deficient manganese dioxides sponge-like 3D architecture for high-performance supercapacitors. Journal of Alloys and Compounds, 2019, 809, 151790.	2.8	11
75	A flexible resistive temperature detector (RTD) based on in-situ growth of patterned Ag film on polyimide without lithography. Microelectronic Engineering, 2019, 216, 111052.	1.1	25
76	Constructing Geneâ€Enhanced Tissue Engineering for Regeneration and Repair of Osteochondral Defects. Advanced Biology, 2019, 3, 1900004.	3.0	1
77	High efficiency and fast van der Waals hetero-photodiodes with a unilateral depletion region. Nature Communications, 2019, 10, 4663.	5.8	213
78	Multifunctional Polydiacetylenic Complex Films: Preferential Host-Guest Interaction with Specific Small Molecules and Recognition of Aldehyde Derivatives. Journal of Nanomaterials, 2019, 2019, 1-6.	1.5	1
79	In situ interface engineering for probing the limit of quantum dot photovoltaic devices. Nature Nanotechnology, 2019, 14, 950-956.	15.6	30
80	Design of Switched-Current Based Low-Power PIM Vision System for IoT Applications. , 2019, , .		1
81	A strategy using mesoporous polymer nanospheres as nanocarriers of Bcl-2 siRNA towards breast cancer therapy. Journal of Materials Chemistry B, 2019, 7, 477-487.	2.9	14
82	AsP/InSe Van der Waals Tunneling Heterojunctions with Ultrahigh Reverse Rectification Ratio and High Photosensitivity. Advanced Functional Materials, 2019, 29, 1900314.	7.8	121
83	Thicknessâ€Dependent Asymmetric Potential Landscape and Polarization Relaxation in Ferroelectric Hf <i>_x</i> Zr _{1â^'} <i>_x</i> O ₂ Thin Films through Interfacial Bound Charges. Advanced Electronic Materials, 2019, 5, 1900554.	2.6	13
84	Substrates and interlayer coupling effects on Mo _{1â^'x} W _x Se ₂ alloys. Journal of Semiconductors, 2019, 40, 062005.	2.0	12
85	A Novel Flexible Silver Heater Fabricated by a Solution-Based Polyimide Metalization and Inkjet-Printed Carbon Masking Technique. ACS Applied Electronic Materials, 2019, 1, 928-935.	2.0	12
86	Hierarchical MoS ₂ Hollow Architectures with Abundant Mo Vacancies for Efficient Sodium Storage. ACS Nano, 2019, 13, 5533-5540.	7.3	187
87	In Situ Interfacial Manipulation of Metastable States Between Nucleation and Decomposition of Single Bismuth Nanoparticle. Physica Status Solidi (B): Basic Research, 2019, 256, 1800442.	0.7	6
88	Structure-Property Relationships in Graphene-Based Strain and Pressure Sensors for Potential Artificial Intelligence Applications. Sensors, 2019, 19, 1250.	2.1	64
89	Characterization of atomic defects on the photoluminescence in twoâ€dimensional materials using transmission electron microscope. InformaÄnÃ-Materiály, 2019, 1, 85-97.	8.5	46
90	Review of Printed Electrodes for Flexible Devices. Frontiers in Materials, 2019, 5, .	1.2	85

#	Article	IF	CITATIONS
91	Dual-Mode Sensor and Actuator to Learn Human-Hand Tracking and Grasping. IEEE Transactions on Electron Devices, 2019, 66, 5407-5410.	1.6	20
92	Raman Characterization on Two-Dimensional Materials-Based Thermoelectricity. Molecules, 2019, 24, 88.	1.7	19
93	A general and facile method for preparation of large-scale reduced graphene oxide films with controlled structures. Carbon, 2019, 143, 162-171.	5.4	30
94	Highly Sensitive and Flexible Tactile Sensor Based on Porous Graphene Sponges for Distributed Tactile Sensing in Monitoring Human Motions. Journal of Microelectromechanical Systems, 2019, 28, 154-163.	1.7	48
95	VSe2/carbon-nanotube compound for all solid-state flexible in-plane supercapacitor. Applied Physics Letters, 2019, 114, .	1.5	34
96	Controlled Doping of Waferâ€6cale PtSe ₂ Films for Device Application. Advanced Functional Materials, 2019, 29, 1805614.	7.8	87
97	Recommended Methods to Study Resistive Switching Devices. Advanced Electronic Materials, 2019, 5, 1800143.	2.6	452
98	Palladium Diselenide Long-Wavelength Infrared Photodetector with High Sensitivity and Stability. ACS Nano, 2019, 13, 2511-2519.	7.3	198
99	In Situ Observation of Crystalline Silicon Growth from SiO ₂ at Atomic Scale. Research, 2019, 2019, 3289247.	2.8	8
100	Interfacial Defects: Probing and Manipulating the Interfacial Defects of InGaAs Dual‣ayer Metal Oxides at the Atomic Scale (Adv. Mater. 2/2018). Advanced Materials, 2018, 30, 1870013.	11.1	1
101	Metallic few-layered VSe ₂ nanosheets: high two-dimensional conductivity for flexible in-plane solid-state supercapacitors. Journal of Materials Chemistry A, 2018, 6, 8299-8306.	5.2	89
102	Preparation, performances and mechanisms of magnetic Saccharomyces cerevisiae bionanocomposites for atrazine removal. Chemosphere, 2018, 200, 380-387.	4.2	75
103	Ultracompact Si-GST Hybrid Waveguides for Nonvolatile Light Wave Manipulation. IEEE Photonics Journal, 2018, 10, 1-10.	1.0	45
104	Atomic Scale Modulation of Selfâ€Rectifying Resistive Switching by Interfacial Defects. Advanced Science, 2018, 5, 1800096.	5.6	29
105	General Synthetic Strategy for Libraries of Supported Multicomponent Metal Nanoparticles. ACS Nano, 2018, 12, 4594-4604.	7.3	66
106	Attapulgite suspension mitigates fine particulate matter (PM2.5) emission from coal combustion in fluidized bed. Journal of Environmental Management, 2018, 209, 245-253.	3.8	6
107	Surface step decoration of isolated atom as electron pumping: Atomic-level insights into visible-light hydrogen evolution. Nano Energy, 2018, 45, 109-117.	8.2	118
108	In situ atomic-scale observation of monolayer graphene growth from SiC. Nano Research, 2018, 11, 2809-2820.	5.8	21

#	Article	IF	CITATIONS
109	Simultaneous atomic-level visualization and high precision photocurrent measurements on photoelectric devices by <i>in situ</i> TEM. RSC Advances, 2018, 8, 948-953.	1.7	7
110	Raman spectroscopy characterization of two-dimensional materials. Chinese Physics B, 2018, 27, 037802.	0.7	38
111	Magnetic bionanoparticles of Penicillium sp. yz11-22N2 doped with Fe3O4 and encapsulated within PVA-SA gel beads for atrazine removal. Bioresource Technology, 2018, 260, 196-203.	4.8	60
112	Combined treatment with Dendrobium candidum and black tea extract promotes osteoprotective activity in ovariectomized estrogen deficient rats and osteoclast formation. Life Sciences, 2018, 200, 31-41.	2.0	9
113	Experimental study on the magnetic characteristics of coal fly ash at different combustion temperatures. Environmental Technology (United Kingdom), 2018, 39, 1967-1975.	1.2	7
114	Probing and Manipulating the Interfacial Defects of InGaAs Dual‣ayer Metal Oxides at the Atomic Scale. Advanced Materials, 2018, 30, 1703025.	11.1	21
115	Properties of graphene-metal contacts probed by Raman spectroscopy. Carbon, 2018, 127, 491-497.	5.4	70
116	RGO-Protected Electroless Plated Nickel Electrode with Enhanced Stability Performance for Flexible Micro-Supercapacitors. ACS Applied Energy Materials, 2018, 1, 7182-7190.	2.5	12
117	Highâ€Performance Waferâ€Scale MoS ₂ Transistors toward Practical Application. Small, 2018, 14, e1803465.	5.2	88
118	Green tea (Camellia sinensis) aqueous extract alleviates postmenopausal osteoporosis in ovariectomized rats and prevents RANKL-induced osteoclastogenesis in vitro. Food and Nutrition Research, 2018, 62, .	1.2	18
119	Integrating the g-C ₃ N ₄ Nanosheet with B–H Bonding Decorated Metal–Organic Framework for CO ₂ Activation and Photoreduction. ACS Nano, 2018, 12, 5333-5340.	7.3	263
120	Interface Designing over WS ₂ /W ₂ C for Enhanced Hydrogen Evolution Catalysis. ACS Applied Energy Materials, 2018, 1, 3377-3384.	2.5	54
121	Probing and manipulating the interfacial defects of InGaAs dual-layer metal oxides at the atomic scale. , 2018, , .		0
122	Efficient removal of atrazine from aqueous solutions using magnetic Saccharomyces cerevisiae bionanomaterial. Applied Microbiology and Biotechnology, 2018, 102, 7597-7610.	1.7	35
123	High-Performance Near-Infrared Photodetectors Based on p-Type SnX (X = S, Se) Nanowires Grown <i>via</i> Chemical Vapor Deposition. ACS Nano, 2018, 12, 7239-7245.	7.3	101
124	Ultrafast Dynamic Pressure Sensors Based on Graphene Hybrid Structure. ACS Applied Materials & Interfaces, 2017, 9, 24148-24154.	4.0	103
125	Ligandâ€Controlled Formation and Photoluminescence Properties of CH ₃ NH ₃ PbBr ₃ Nanocubes and Nanowires. ChemNanoMat, 2017, 3, 303-310.	1.5	57
126	Synthesis of zeolite-like metal–organic frameworks via a dual-ligand strategy. CrystEngComm, 2017, 19, 2549-2552.	1.3	11

#	Article	IF	CITATIONS
127	A high-performance flexible piezoelectric energy harvester based on lead-free (Na ₀ . ₅ 8i ₀ . ₅)TiO ₃ –BaTiO ₃ piezoelectric nanofibers. Journal of Materials Chemistry A, 2017, 5, 23634-23640.	5.2	48
128	In Situ Transmission Electron Microscopy Characterization and Manipulation of Twoâ€Dimensional Layered Materials beyond Graphene. Small, 2017, 13, 1604259.	5.2	75
129	The Relationship between Regional Gray Matter Volume of Social Exclusion Regions and Personal Self-Esteem Is Moderated by Collective Self-Esteem. Frontiers in Psychology, 2017, 8, 1989.	1.1	3
130	Catenation of Homochiral Metal–Organic Nanocages or Nanotubes. Inorganic Chemistry, 2016, 55, 5095-5097.	1.9	14
131	Visible Light-Assisted High-Performance Mid-Infrared Photodetectors Based on Single InAs Nanowire. Nano Letters, 2016, 16, 6416-6424.	4.5	134
132	Universal route to fabricate facile and flexible micro-supercapacitors with gold-coated silver electrodes. RSC Advances, 2016, 6, 81936-81942.	1.7	6
133	Hotâ€Electrons Mediated Efficient Visibleâ€Light Photocatalysis of Hierarchical Black Au–TiO ₂ Nanorod Arrays on Flexible Substrate. Advanced Materials Interfaces, 2016, 3, 1600588.	1.9	26
134	Zeeman splitting and dynamical mass generation in Dirac semimetal ZrTe5. Nature Communications, 2016, 7, 12516.	5.8	149
135	Analysis of nano-filament evolution in Ni-based RRAM devices using in-situ TEM. , 2016, , .		0
136	Compliance current dominates evolution of NiSi2 defect size in Ni/dielectric/Si RRAM devices. Microelectronics Reliability, 2016, 61, 71-77.	0.9	13
137	When Nanowires Meet Ultrahigh Ferroelectric Field–High-Performance Full-Depleted Nanowire Photodetectors. Nano Letters, 2016, 16, 2548-2555.	4.5	135
138	Liquid-phase epitaxial growth of a homochiral MOF thin film on poly(<scp>I</scp> -DOPA) functionalized substrate for improved enantiomer separation. Chemical Communications, 2016, 52, 772-775.	2.2	60
139	Complete mitochondrial genome of <i>Vaginulus alte</i> and <i>Homoiodoris japonica</i> . Mitochondrial DNA Part A: DNA Mapping, Sequencing, and Analysis, 2016, 27, 3454-3457.	0.7	4
140	Polarization fluctuation behavior of lanthanum substituted Bi4Ti3O12 thin films. Journal of Applied Physics, 2015, 118, 104102.	1.1	18
141	Evolution of Filament Formation in Ni/HfO ₂ /SiO <i>_x</i> /Siâ€Based RRAM Devices. Advanced Electronic Materials, 2015, 1, 1500130.	2.6	37
142	Sizeâ€Dependent Enantioselective Adsorption of Racemic Molecules through Homochiral Metal–Organic Frameworks Embedding Helicity. Chemistry - A European Journal, 2015, 21, 10236-10240.	1.7	29
143	Graphene and Other 2D Material Components Dynamic Characterization and Nanofabrication at Atomic Scale. Journal of Nanomaterials, 2015, 2015, 1-6.	1.5	1
144	A single iron site confined in a graphene matrix for the catalytic oxidation of benzene at room temperature. Science Advances, 2015, 1, e1500462.	4.7	719

#	Article	IF	CITATIONS
145	Two-Dimensional Layered Materials-Based Spintronics. Spin, 2015, 05, 1540011.	0.6	10
146	Cu–Al intermetallic compound investigation using ex-situ post annealing and in-situ annealing. Microelectronics Reliability, 2015, 55, 2316-2323.	0.9	11
147	Repetitive-Avalanche-Induced Electrical Parameters Shift for 4H-SiC Junction Barrier Schottky Diode. IEEE Transactions on Electron Devices, 2015, 62, 601-605.	1.6	25
148	Synthesis and gas sorption properties of a homochiral metal–organic framework with octahedral cages. CrystEngComm, 2015, 17, 6107-6109.	1.3	9
149	Construction of hierarchical CoS nanowire@NiCo ₂ S ₄ nanosheet arrays via one-step ion exchange for high-performance supercapacitors. Journal of Materials Chemistry A, 2015, 3, 24033-24040.	5.2	119
150	A facile approach for the synthesis of highly luminescent carbon dots using vitamin-based small organic molecules with benzene ring structure as precursors. RSC Advances, 2015, 5, 90245-90254.	1.7	60
151	Asymmetric induction in homochiral MOFs: from interweaving double helices to single helices. Chemical Communications, 2015, 51, 16331-16333.	2.2	34
152	Facile ion-exchange synthesis of silver films as flexible current collectors for micro-supercapacitors. Journal of Materials Chemistry A, 2015, 3, 21009-21015.	5.2	24
153	ZnSeâ€Based Longitudinal Twinning Nanowires. Advanced Engineering Materials, 2014, 16, 459-465.	1.6	18
154	Identification and application of radiation-related microRNAs. Rendiconti Lincei, 2014, 25, 49-52.	1.0	0
155	Synthesis and Optical Properties of Largeâ€Area Singleâ€Crystalline 2D Semiconductor WS ₂ Monolayer from Chemical Vapor Deposition. Advanced Optical Materials, 2014, 2, 131-136.	3.6	513
156	Silicon carbide-derived carbon nanocomposite as a substitute for mercury in the catalytic hydrochlorination of acetylene. Nature Communications, 2014, 5, 3688.	5.8	181
157	Direct, Nonoxidative Conversion of Methane to Ethylene, Aromatics, and Hydrogen. Science, 2014, 344, 616-619.	6.0	1,113
158	Carbon Microbelt Aerogel Prepared by Waste Paper: An Efficient and Recyclable Sorbent for Oils and Organic Solvents. Small, 2014, 10, 3544-3550.	5.2	196
159	Dynamic investigation of interface atom migration during heterostructure nanojoining. Nanoscale, 2014, 6, 405-411.	2.8	9
160	Defect-mediated phase transition temperature of VO2 (M) nanoparticles with excellent thermochromic performance and low threshold voltage. Journal of Materials Chemistry A, 2014, 2, 4520.	5.2	90
161	Comparative studies of redox behaviors of Pt–Co/SiO ₂ and Au–Co/SiO ₂ catalysts and their activities in CO oxidation. Catalysis Science and Technology, 2014, 4, 3151-3158.	2.1	26
162	Raman mapping investigation of chemical vapor deposition-fabricated twisted bilayer graphene with irregular grains. Physical Chemistry Chemical Physics, 2014, 16, 21682-21687.	1.3	23

#	Article	IF	CITATIONS
163	Tunable Electroluminescence in Planar Graphene/SiO ₂ Memristors. Advanced Materials, 2013, 25, 5593-5598.	11.1	67
164	Advanced methodologies for atomic-scale nanofabrication and dynamic characterization. , 2013, , .		0
165	Feasibility of SILC Recovery in Sub-10-à EOT Advanced Metal Gate–High-\$kappa\$ Stacks. IEEE Electron Device Letters, 2013, 34, 1053-1055.	2.2	8
166	<i>In situ</i> observation of nickel as an oxidizable electrode material for the solid-electrolyte-based resistive random access memory. Applied Physics Letters, 2013, 102, .	1.5	65
167	Intrinsic nanofilamentation in resistive switching. Journal of Applied Physics, 2013, 113, 114503.	1.1	69
168	Layer-by-Layer Thinning of MoS ₂ by Plasma. ACS Nano, 2013, 7, 4202-4209.	7.3	387
169	Top–down fabrication of sub-nanometre semiconducting nanoribbons derived from molybdenum disulfide sheets. Nature Communications, 2013, 4, 1776.	5.8	220
170	Graphene Scaffolds Enhanced Photogenerated Electron Transport in ZnO Photoanodes for High-Efficiency Dye-Sensitized Solar Cells. Journal of Physical Chemistry C, 2013, 117, 8619-8627.	1.5	69
171	Evolution of Raman spectra in nitrogen doped graphene. Carbon, 2013, 61, 57-62.	5.4	228
172	Resilience of ultra-thin oxynitride films to percolative wear-out and reliability implications for high-l [̂] stacks at low voltage stress. Journal of Applied Physics, 2013, 114, 094504.	1.1	8
173	Dielectric breakdown — Recovery in logic and resistive switching in memory — Bridging the gap between the two phenomena. , 2012, , .		2
174	The neural basis of impossible figures: Evidence from an fMRI study of the two-pronged trident. Neuroscience Letters, 2012, 508, 17-21.	1.0	2
175	Percolative Model and Thermodynamic Analysis of Oxygen-Ion-Mediated Resistive Switching. IEEE Electron Device Letters, 2012, 33, 712-714.	2.2	19
176	Filamentation Mechanism of Resistive Switching in Fully Silicided High- \$kappa\$ Gate Stacks. IEEE Electron Device Letters, 2011, 32, 455-457.	2.2	13
177	Oxygen-Soluble Gate Electrodes for Prolonged High-\$ kappa\$ Gate-Stack Reliability. IEEE Electron Device Letters, 2011, 32, 252-254.	2.2	20
178	Physical analysis of breakdown in high-κ/metal gate stacks using TEM/EELS and STM for reliability enhancement (invited). Microelectronic Engineering, 2011, 88, 1365-1372.	1.1	19
179	Evidence for compliance controlled oxygen vacancy and metal filament based resistive switching mechanisms in RRAM. Microelectronic Engineering, 2011, 88, 1124-1128.	1.1	44
180	Using post-breakdown conduction study in a MIS structure to better understand the resistive switching mechanism in an MIM stack. Nanotechnology, 2011, 22, 455702.	1.3	12

#	Article	IF	CITATIONS
181	Uncorrelated multiple conductive filament nucleation and rupture in ultra-thin high-κ dielectric based resistive random access memory. Applied Physics Letters, 2011, 99, 093502.	1.5	24
182	On the Study of Radio Resource Allocation of Heterogeneous Services with Soft QoS Traffics in OFDMA-based Wireless Networks. , 2010, , .		0
183	Characterization of Pinhole in Patterned Oxide Buried in Bonded Silicon-on-Insulator Wafers by Near-Infrared Scattering Topography and Transmission Microscopy. Journal of the Electrochemical Society, 2008, 155, H864.	1.3	0
184	Characterization of Patterned Oxide Buried in Bonded Silicon-on-Insulator Wafers by Near-Infrared Scattering Topography and Microscopy. Japanese Journal of Applied Physics, 2008, 47, 2511-2514.	0.8	0
185	Experimental Study on Capture of PM10 Emitted from Coal Combustion with High Gradient Magnetic Field. AIP Conference Proceedings, 2007, , .	0.3	3
186	AC-based Capacitance Tomography System With Small-diameter And High-pressure Pipe. AIP Conference Proceedings, 2007, , .	0.3	0
187	Experimental investigation on agglomeration of coal-fired PM10 in uniform magnetic field. AIP Conference Proceedings, 2007, , .	0.3	Ο
188	Nonlinear Image Reconstruction Using a GA-ECT Technique in Electrical Capacitance Tomography. AIP Conference Proceedings, 2007, , .	0.3	3
189	Characterization of Pinhole in Patterned Oxide Buried in Bonded Silicon-on-Insulator Wafers by Near-Infrared Scattering Topography and Microscopy. ECS Transactions, 2007, 11, 173-182.	0.3	1
190	Aggregation mechanism of fine fly ash particles in uniform magnetic field. Korean Journal of Chemical Engineering, 2007, 24, 319-327.	1.2	18
191	Desulfurization in reducing atmosphere and ammonia injection denitrification in a coal-fired fluidized bed combustor with fly-ash recycle. Journal of Thermal Science, 1997, 6, 75-79.	0.9	3
192	Linear FM/chirped radar receiver matched filter implementation. , 0, , .		0
193	A novel approach for CFAR processors design. , 0, , .		15
194	Chaotic phase code for radar pulse compression. , 0, , .		24
195	Sidelobe suppression using adaptive filtering techniques. , 0, , .		4